

# Growth cone response to ephrin gradients produced by microfluidic networks

Susanne Lang · Anne C. von Philipsborn ·  
André Bernard · Friedrich Bonhoeffer ·  
Martin Bastmeyer

Received: 3 April 2007 / Revised: 3 May 2007 / Accepted: 10 May 2007 / Published online: 8 June 2007  
© Springer-Verlag 2007

**Abstract** A microfluidic network ( $\mu$ FN) etched into a silicon wafer was used to deliver protein solutions containing different concentrations of the axonal guidance molecule ephrinA5 onto a silicone stamp. In a subsequent microcontact printing ( $\mu$ CP) step, the protein was transferred onto a polystyrene culture dish. In this way, stepwise substrate-bound concentration gradients of ephrinA5 were fabricated spanning a total distance of 320  $\mu$ m. We tested the response of chick retinal ganglion cell (RGC) axons, which are guided in vivo by ephrin gradients, to these in vitro gradients. Temporal, but not nasal axons stop at a distinct zone in the gradient, which is covered with a certain surface density of substrate-bound ephrinA5. Within the temporal RGC population, all axons respond uniformly to the gradients tested. The position of the stop zone depends on the slope of the gradient with axons growing further into

the gradient in shallow gradients than in steep gradients. However, axons stop at lower ephrinA5 concentrations in shallow gradients than in steep gradients, indicating that the growth cone can adjust its sensitivity during the detection of a concentration gradient of ephrinA5.

**Keywords** Microfluidic network · Microcontact printing · Axon guidance · Retinotectal projection · Chick · Ephrin

## Abbreviations

$\mu$ FN microfluidic network  
 $\mu$ CP microcontact printing  
RGC retinal ganglion cell  
PDMS polydimethylsiloxane

## Introduction

During development the nervous system is built up with the help of guidance molecules, which direct axonal outgrowth and neuronal connectivity [1, 2]. A number of these guidance molecules are distributed in a graded way and therefore convey both directional and positional information. The graded distribution of a guidance cue in a target region and the graded expression of the corresponding receptor on the ingrowing axons can drive the formation of topographic maps, which consist of a population of projecting neurons, whose axonal connections in the target region reflect their original spatial order [3]. One of the best-studied neural topographic maps is the connection between the vertebrate eye and the brain, the retinotectal/collicular projection [4–7]. Retinal ganglion cells (RGCs) axons from the temporal retina expressing high levels of EphA receptors are confined to the anterior tectum

Susanne Lang and Anne C. von Philipsborn contributed equally to this work: S.L. performed the experiments; A.P. evaluated the data and wrote the paper.

S. Lang · F. Bonhoeffer  
Max-Planck-Institut für Entwicklungsbiologie,  
Spemannstraße 35,  
72076 Tübingen, Germany

A. C. von Philipsborn · M. Bastmeyer (✉)  
Zoologisches Institut I, Zell- und Neurobiologie,  
Universität Karlsruhe (TH),  
Haid- und Neu- Straße 9,  
76131 Karlsruhe, Germany  
e-mail: bastmeyer@bio.uka.de

A. Bernard  
Institut für Mikro- und Nanotechnologie,  
Interstaatliche Hochschule für Technik Buchs NTB,  
Werdenbergstraße 4,  
9471 Buchs, Switzerland

containing low levels of the repulsive guidance molecule ephrinA, whereas nasal RGC axons with less EphA receptor invade the ephrinA gradient in the target region up to the posterior part of the tectum [8–10]. EphrinA gradients are also expressed in a nasal low to temporal high orientation in the retina; and EphA gradients are expressed in a posterior high to anterior low orientation in the tectum. This second set of receptor–ligand gradients also participates in retinotectal mapping [11, 12]. In the present study, we solely consider the response of EphA-bearing RGC growth cones to gradients of purified ephrinA5.

So far, it is not fully understood how concentration gradients of guidance factors are detected and processed by the tip of a growing axon, the nerve growth cone. Most *in vitro* data come from studies with diffusible gradients of guidance factors, which can elicit repulsive and attractive turning responses of the growth cone [13, 14]. However, most guidance factors in the nervous system are bound to cell membranes or the extracellular matrix. In the case of ephrinA, membrane attachment and/or clustering are required for proper Eph receptor activation [15, 16]. For the comprehensive study of axonal gradient detection it is therefore essential to fabricate substrate-bound concentration gradients of guidance molecules *in vitro*.

To obtain highly reproducible and long-lasting graded distributions of purified ephrinA5, microcontact printing ( $\mu$ CP) [17] proved to be a useful technique. Gradients fabricated by  $\mu$ CP are discontinuous on a microscale, i.e. they consist of an increasingly denser pattern of protein dots or lines. These vary with respect to size and spacing but are covered by the same protein concentration [18, 19].

In the present work, we used a  $\mu$ FN [20, 21] to transmit different protein concentrations onto a polystyrene surface in a defined way, resulting in stepwise substrate-bound concentration gradients of ephrinA5. Temporal RGC axons invading these gradients stop in a defined zone within the gradient in a manner that is dependent on the slope of the gradient. The ephrinA5 concentration evoking growth cone stop is lower in shallow gradients than in steep gradients. Growth cones are thus able to distinguish between different gradients and presumably adjust their sensitivity according to the encountered ephrinA5 concentrations.

## Materials and methods

### $\mu$ FN fabrication

The thermal oxide (1- $\mu$ m thick) on top of a Si{100} wafer (4", 525- $\mu$ m thick, Siltronic, Switzerland) was structured by photolithography (photoresist (PR) AZ6612 (Hoechst, France) for 45 s at 4,000 rpm, prebaked at 110 °C for 50 s, exposed through a mask featuring all the elements (ports

and microchannels), developed in AZ400K (Hoechst) diluted 1:4 with deionized water (ddH<sub>2</sub>O), and rinsed in ddH<sub>2</sub>O). The uncovered SiO<sub>2</sub> was then etched away in a 1:7 buffered hydrofluoric acid solution (ca. 15 min). An O<sub>2</sub>-plasma or acetone was used to ash or strip the remaining PR. A second PR layer (AZ4562, Hoechst) was applied (1,500 rpm for 45 s), yielding a thick overlayer of  $\approx$ 10  $\mu$ m. The SiO<sub>2</sub> pattern underneath this PR layer was still visible and was used to align the wafer with a second mask featuring the ports only. After exposure and development of the PR, the wafer was rinsed, dried and postbaked (95 °C, 20 min). An inductively coupled plasma (ICP) DRIE (Surface Technology Systems, Bristol, UK) was used to transfer the PR and embedded SiO<sub>2</sub> patterns into wafer topography in a three-step process: (i) DRIE to make  $\approx$ 250- $\mu$ m-deep ports into Si (pattern defined by the thick PR); (ii) without unloading the wafer from the DRIE machine, the PR was ashed using an O<sub>2</sub>-plasma; (iii) the exposed SiO<sub>2</sub> pattern acts as mask for a second dry-etch process of about 50- $\mu$ m depth, creating the channels connected to the 300- $\mu$ m-deep filling and venting ports. The micromachined wafer was then cleaned with acetone, ethanol and ddH<sub>2</sub>O, and cleaved into individual  $\mu$ FNs.

### Fabrication of substrate-bound protein gradients

A cuboid of polydimethylsiloxane (PDMS, Sylgard 184, Dow Corning, Midland, MI, USA) was trimmed to the appropriate size and placed onto the parallel channel system etched into the silicon wafer, sealing the surface and creating separate channels for fluid flow. The filling ports were left freely accessible. The channels were subsequently filled with 0.2–0.5  $\mu$ L protein solution each with the help of a cut microloader tip (Fig. 1a). In order to ensure ideal conditions during the filling of the  $\mu$ FN and avoid desiccation or condensation, it was placed onto a Peltier module adjusted to 5 °C above the dew point. After the filling procedure, the  $\mu$ FN was incubated for 10–15 min allowing physical adsorption of the protein in the channels onto the PDMS surface. The filling ports were briefly rinsed with ddH<sub>2</sub>O and dried with a stream of N<sub>2</sub>. The filling ports and the channels were then washed for 3 min with blocking solution (5  $\mu$ g mL<sup>-1</sup> BSA in PBS). The PDMS cuboid was carefully lifted, letting the blocking solution flow under the cuboid. The cuboid was rinsed with ddH<sub>2</sub>O, dried with a stream of N<sub>2</sub> and stamped onto a polystyrene cell culture dish (Nunc), thus transferring the adsorbed protein from the PDMS surface onto the polystyrene surface (Fig. 1b). The silicon wafer was then washed with 50% EtOH in ddH<sub>2</sub>O and 100% EtOH, dried and cleaned for 1 min in an O<sub>2</sub>-plasma (pressure 0.8 torr, load coil power 250 W; Technics Plasma 100-E, TePla AG, Germany). The printed protein pattern on the culture dish

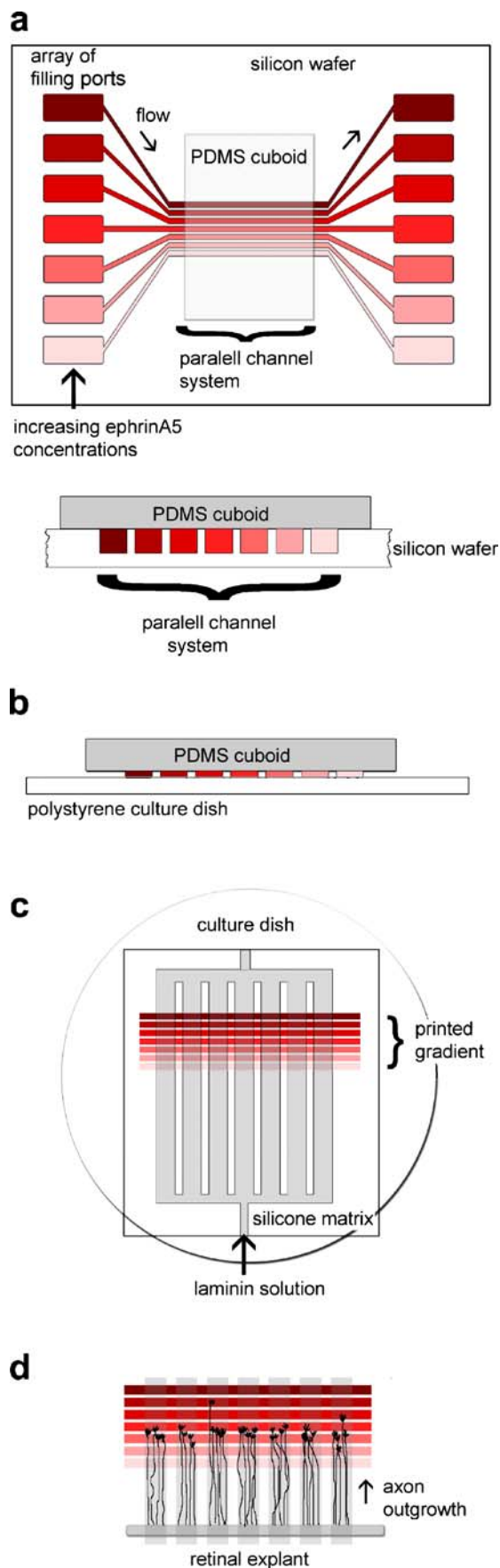


**Fig. 1** Fabrication of graded surface-bound protein patterns by microfluidic networks. **a** A parallel channel system etched into a silicon wafer is sealed by a flat, unstructured PDMS cuboid and filled via separate filling ports with solutions of increasing ephrinA5 concentrations (*red*). During incubation, the protein in solution binds to the PDMS surface. **b** The PDMS cuboid is used as a stamp to transfer the adsorbed protein onto a polystyrene dish. **c** The printed ephrin pattern is covered with a silicone matrix, which is filled with laminin solution (*grey*). The surface is thus coated with laminin in a striped way. **d** The superimposed laminin lanes (*grey*) direct axons outgrowing from a retinal explant into the graded ephrin pattern (*red*)

was overlaid with laminin stripes perpendicular to the ephrin lanes in order to ensure straight outgrowth of the axons. For this, a PDMS matrix containing an array of 40- $\mu\text{m}$ -wide channels separated by 40- $\mu\text{m}$ -wide barriers [22] was placed onto the dish, and filled with 20  $\mu\text{g mL}^{-1}$  laminin (Invitrogen) in PBS (Fig. 1c). After incubation for 30 min, the matrix was flushed with Hanks medium and removed. Before tissue culture, the protein substrates were equilibrated with F12 medium.

For filling the  $\mu\text{FN}$  channels, PBS solutions containing recombinant ephrinA5-Fc chimeric protein (R&D systems) clustered in a mass ratio 1:3 with Alexa Fluor 594 anti-human Fc antibody (Molecular probes) were used. Ephrin concentrations ranged from 9.4 to 150  $\mu\text{g mL}^{-1}$ . All protein solutions were adjusted to a total protein content of 150  $\mu\text{g mL}^{-1}$  by adding Fc (Human IgG, Fc fragment, Calbiochem) clustered with Alexa Fluor 488 anti-human Fc antibody (Molecular probes). Clustered Fc was also used for control experiments.

The fluorescence of the produced patterns was measured as described below in order to check the slope of the gradient. Patterns with irregularities such as missing channels were excluded from the quantitative evaluation.

#### Preparation, fixation and staining of RGC cultures

RGC explants were dissected and cultured according to the method previously described [23]. Briefly, retinae of E 6–7 chick embryos were dissected in Hanks medium and cut along the naso-temporal axis in 275- $\mu\text{m}$ -wide strips. The retinal strips were placed approximately 500  $\mu\text{m}$  in front of the protein patterns (Fig. 1d) and grown in F12 medium containing 0.4% methylcellulose, 2% chicken serum and 5% fetal calf serum (FCS).

After 24 h, the retinal ganglion cell explants were fixed for 30 min in 4% paraformaldehyde/0.1% glutaraldehyde in PBS containing 0.3 M sucrose and stained with Alexa Fluor 647 phalloidin (Molecular Probes). Cultures were embedded in embedding agent (Mowiol, Calbiochem) and photographed with a confocal microscope (Leica TCS SP2). The acquired pictures were further processed with Photoshop CS software (Adobe).

## Quantitative evaluation of axonal growth

The temporal half of the retina was divided in seven segments ranging from the optic fissure (position t1) to the most temporal part of the retina (position t7). Each position included an approximately 400- $\mu\text{m}$ -wide section of the retina. The axonal outgrowth into the gradients was separately analysed for each segment.

The quantitative evaluation of axonal outgrowth was essentially performed as described previously [18]. The fluorescence of the anti-Fc antibody labelling the substrate-bound ephrinA5 and the fluorescence of the phalloidin-stained axons was measured in a 406- $\mu\text{m}$ -wide field containing the protein pattern and an 80- $\mu\text{m}$ -long area preceding the pattern. For this, a 7- $\mu\text{m}$ -long measuring rectangle extending over the entire width of the field was moved in 0.4- $\mu\text{m}$  steps in the direction of axonal growth, i.e. parallel to the gradient over the field, resulting in 1,009 data points along the vertical axis for ephrin and axonal fluorescence. The intensity of axonal fluorescence was plotted against the distance overgrown by the axons, resulting in curves, which reflect the distribution of axons and growth cones in and in front of the printed pattern. After subtracting the background fluorescence, curves were smoothed by calculating the rolling average over 61 data points and normalized for better comparison.

To obtain a mean growth curve for axons of each retinal position in the two different gradients (steep/shallow), the growth curves of the single experiments were added and divided by the number of experiments. As a reference, curves were compared with the arithmetic mean of the relative fluorescence. The mean stop point position in each pattern was defined as the intersection between the axonal growth curve and the arithmetic mean. The standard error of the mean stop point position was calculated based on the stop points of the single experiments.

## Results and discussion

### Characterization of gradients produced by $\mu\text{FN}$

We fabricated two different stepwise gradients using the  $\mu\text{FN}$  described above. For a steep gradient, the first channel was filled with a protein solution containing  $9.4 \mu\text{g mL}^{-1}$  ephrinA5 and  $140.6 \mu\text{g mL}^{-1}$  Fc, resulting in an absolute protein concentration of  $150 \mu\text{g mL}^{-1}$ . In each subsequent channel, the ephrinA5 concentration was increased by  $9.4 \mu\text{g mL}^{-1}$  and the Fc concentration was adjusted accordingly to keep the absolute concentration constant. For a shallow gradient, each of the ephrinA5 solutions used for fabrication of the steep gradient was filled in two adjoining channels (Fig. 2a). To estimate the average

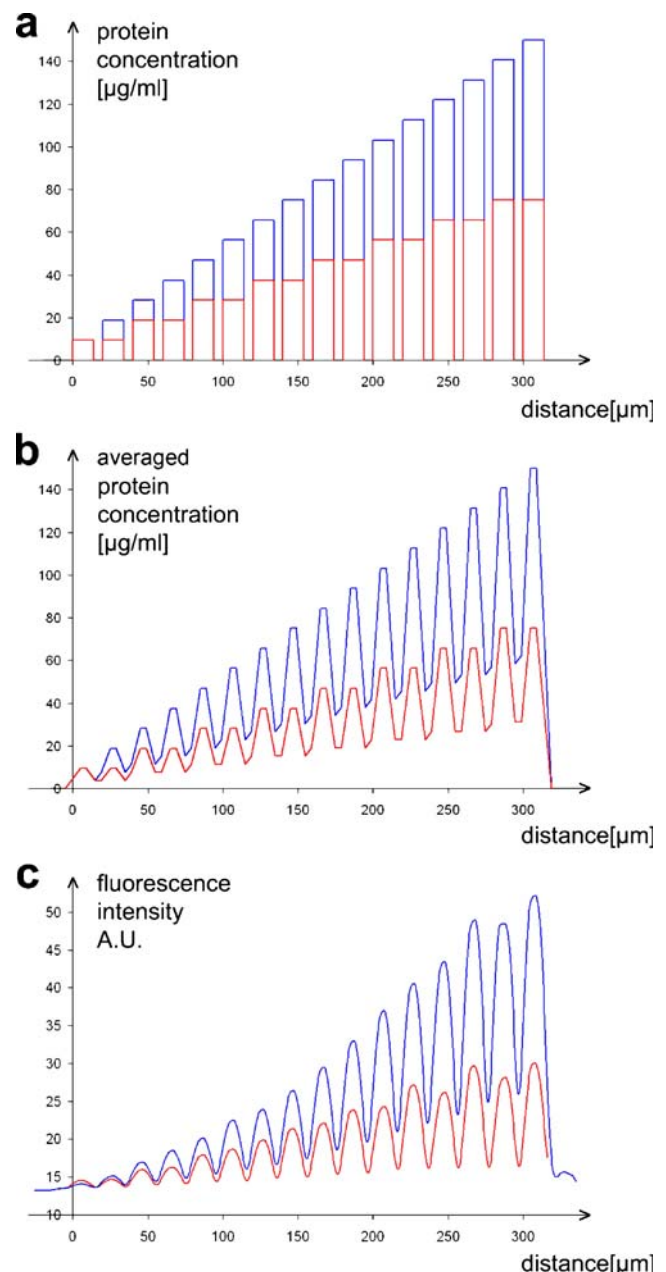


**Fig. 2** Stepwise gradients produced by  $\mu\text{FN}$ . **a** Protein concentrations added into the  $\mu\text{FN}$  channels in order to produce a steep (blue) and a shallow (red) gradient. **b** Protein concentrations encountered by a theoretical growth cone, averaging the ephrin concentration over its length (7  $\mu\text{m}$ ). **c** Fluorescence intensity of the antibody-labelled surface-bound ephrinA5 on the polystyrene dish, measured by a rolling average over 7  $\mu\text{m}$ . The curves are the mean of  $n=9$  (steep gradient) and  $n=20$  (shallow gradient) evaluated patterns

ephrinA5 concentrations encountered by a growth cone, we assumed that it integrates the ephrinA5 under its surface area. Since a growth cone is approximately 7- $\mu\text{m}$  long, we calculated the average protein concentration in a 7- $\mu\text{m}$ -long measuring rectangle moving along the axis of the gradient. The resulting distribution illustrates that the outgrowing



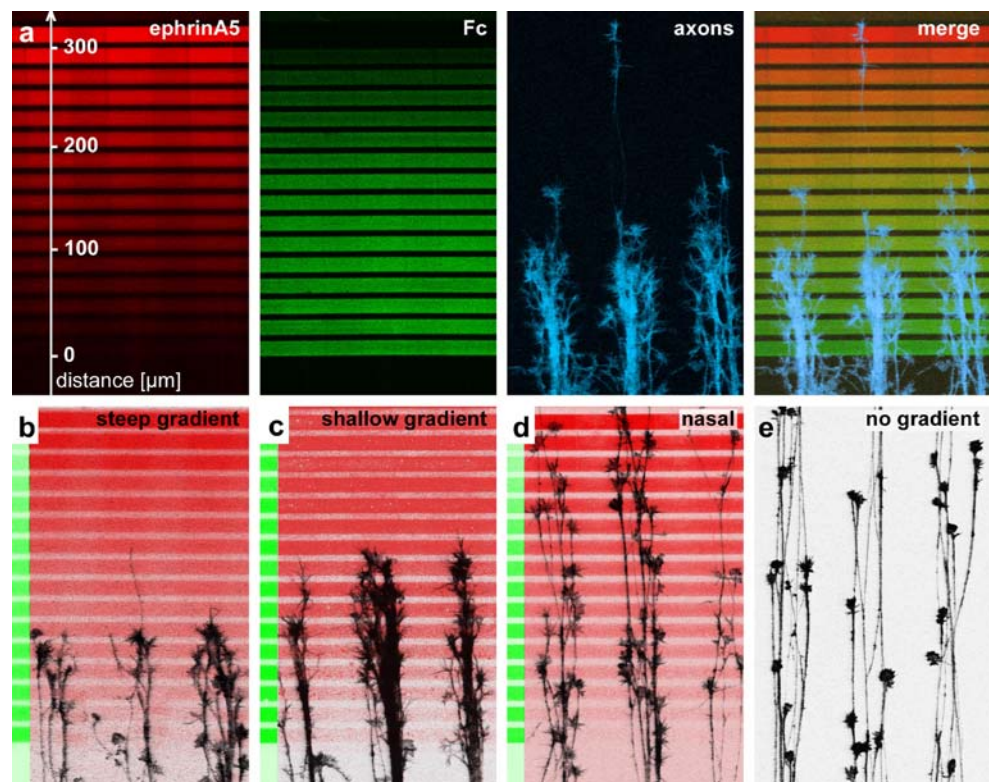
axons are faced with a undulating increase of concentration (Fig. 2b). To evaluate how the concentration of the protein solutions added into the  $\mu$ FN channels corresponds to the amount of ephrinA5 bound to the surface of the culture dish, we measured the fluorescence intensity of the antibody-clustered ephrinA5 by moving a 7- $\mu$ m-long measuring rectangle along the axis of the gradient. As shown in Fig. 2c, the fluorescence intensity of the labelled protein bound to the surface is roughly proportional to the protein concentration of the solutions in the channel system and can be used to check the quality of the produced pattern.

#### Temporal RGC axons stop in ephrinA5 gradients produced by $\mu$ FNs

In order to test the response of RGC axons to stepwise ephrinA5 gradients, retinal explants were placed 500–700  $\mu$ m in front of the gradients. After 24 h, when axons had exited the explant and grown on the laminin-covered lanes perpendicular to the gradient, the cultures were fixed and stained. Temporal RGC axons invade the beginning of the gradient, but do not advance beyond a certain point. Most growth cones stop at a defined zone in the gradient (Fig. 3a–c). Since axons grow laterally confined on the laminin-covered lanes, they tend to have a fasciculated

aspect. Many axons in a single laminin lane simultaneously arrive at the stop zone, and the invasion of the gradient as well as the stop reaction are not preceded by a few pioneer axons. Stopping growth cones do not collapse or retract, but pause with intact filopodia and lamellipodia within the stop zone. Stop zones become apparent after 18–20 h and stay stable for up to 2 days in culture. Temporal axons stop after a shorter overgrown distance in steep gradients than in shallow gradients (Fig. 3b,c). In contrast to temporal axons, nasal axons overgrow the ephrinA5 gradients without stopping (Fig. 3d) and have essentially the same distribution as axons growing outside the gradient on a striped laminin substrate (Fig. 3e). The lack of a stop reaction with nasal axons in substrate-bound ephrinA5 gradients was also observed in gradients produced by  $\mu$ CP [18] and contrasts with the findings that nasal axons are sensitive to high concentrations of ephrinA5 in the growth cone collapse or stripe assay [24]. We conclude that persistent growth cone stop in substrate-bound ephrinA5 gradients requires high sensitivity of the growth cone and is a cellular process different from growth cone collapse in the presence of soluble ephrinA5 as well as from the avoidance response to ephrinA5 lanes parallel to the growth direction in the stripe assay. Patterns in which all lanes are covered with 150  $\mu$ g mL<sup>-1</sup> Fc affect neither temporal nor nasal axons (data not shown).

**Fig. 3** Temporal RGC axons stop in substrate-bound gradients produced by  $\mu$ FN. **a** Fluorescence images of a stepwise gradient of ephrinA5 spanning a distance of 320  $\mu$ m, the corresponding countergradient of Fc and temporal axons stained with phalloidin invading the gradient. In **b–e** phalloidin-stained axons are shown in *black*, antibody stained ephrin in *red* and antibody stained Fc in *green*. **b** Temporal axons stopping in a steep ephrinA5 gradient. **c** The stop zone shifts further into the gradient in a shallow gradient. **d** Nasal axons in a steep gradient do not stop. **e** Temporal axons growing on laminin lanes without underlying gradient. For scale, see **a**



Temporal RGC axons stop at lower ephrinA5 concentration in shallow gradients than in steep gradients

For quantitative evaluation of the axonal stop reaction (see [Materials and methods](#)), the axonal fluorescence was measured for all experiments and axonal growth curves were used to determine the position of the stop zone. Figure 4a shows the two average axonal growth curves for the shallow and the steep gradient, respectively, illustrating that the mean axonal stop position in the steep gradient is located in the sixth lane of the gradient, whereas it is located in the eighth lane in the shallow gradient. The analysis of single experiments confirms that the stop response in the shallow gradient ( $161.0 \pm 5.2 \mu\text{m}$ ;  $n=84$ ) is clearly distinct from that in the steep gradient ( $110.3 \pm 3.8 \mu\text{m}$ ;  $n=48$ ) ( $P < 0.001$  by Student's *t*-test). The sixth lane of the steep gradient corresponds to a  $\mu\text{FN}$  channel filled with  $56.3 \mu\text{g mL}^{-1}$  ephrinA5 solution and the eighth lane of the shallow gradient to a channel filled with  $37.5 \mu\text{g mL}^{-1}$  ephrinA5 solution. Since the concentration of the protein solution added into the  $\mu\text{FN}$  channels is assumed to be directly proportional to the amount of surface-bound ephrinA5, we conclude that temporal axons thus stop at a lower ephrinA5 concentration in the shallow gradient (2/3 of the concentration at the stop position in steep gradients).

Since axons overgrow a longer distance in the shallow gradients, one could assume that they have encountered a

higher total amount of surface-bound ephrinA5 and thus stop a lower local ephrinA5 concentration in exchange. However, this is not the case, since axons stop in shallow gradients after having overgrown a slightly lower total amount of surface-bound ephrinA5. If the total amount of ephrinA5 encountered up to the sixth lane in a steep gradient is set at 100 arbitrary units (A.U.), axons stopping at the eighth lane in a shallow gradient have only encountered 95 A.U. of surface-bound ephrinA5 on their way up to the stop position.

Taken together, temporal axons are more sensitive toward shallow gradients than steep gradients. Since the growth cone is able to adapt to guidance factors, i.e. to adjust its responsiveness according to the signal strength [25, 26], this finding could be explained by a potentially lower rate of adaptation/desensitization in shallow gradients. A similar relation between gradient slope and the ephrin concentration at the axonal stop zone was also found for discontinuous gradients produced by  $\mu\text{CP}$ , where axons stop in areas with a lower percentage of ephrin coverage in shallow graded patterns than in steep ones [18].

Since the average velocity of a growth cone is about  $2, 4 \mu\text{m min}^{-1}$ , it takes approximately 45 min to reach the stop zone position in a steep gradient and 70 min in a shallow gradient. These time frames are likely to be sufficient for an adaptation process, since growth cone adaptation to guidance factors has been previously reported to occur, depending on the experimental assay,

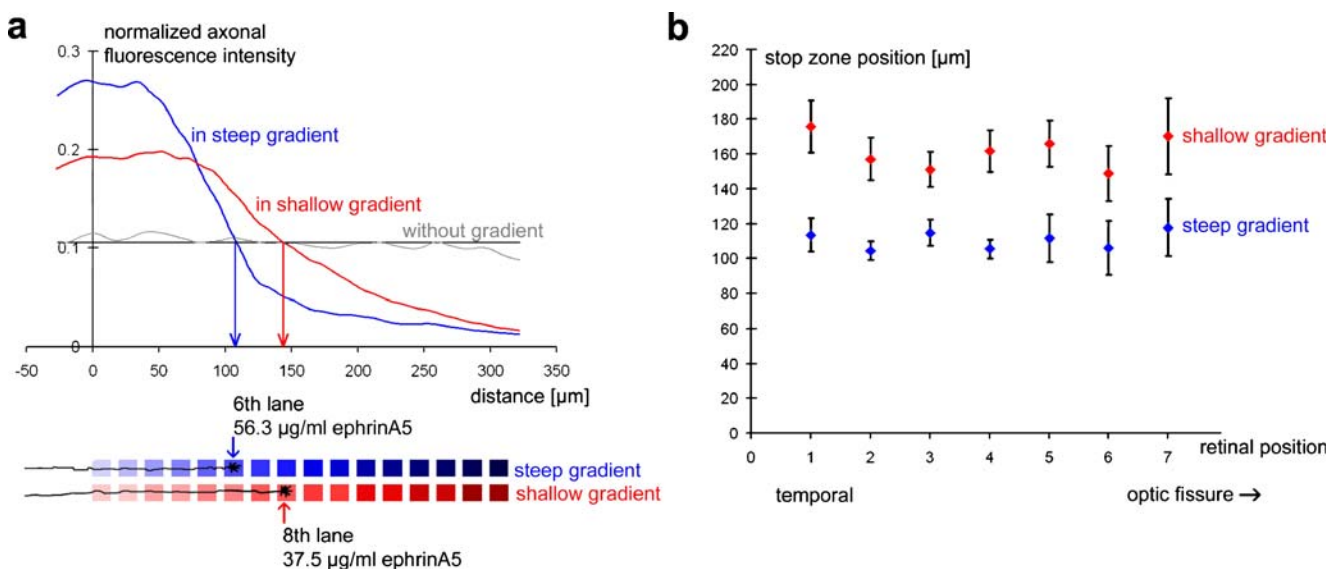


**Fig. 4** Temporal RGC axons can distinguish between different gradient slopes. **a** Stop zone positions of temporal axons in the steep and the shallow gradients were determined by measuring the normalized axonal fluorescence intensity along the axis of the gradient. The blue curve represents the mean normalized axonal fluorescence intensity in the steep gradient, the red curve in the shallow gradient. The grey curve represents the axonal fluorescence intensity outside a gradient runs close to the arithmetic mean (black

line). The curves were averaged from  $n=48$  (steep gradient),  $n=84$  (shallow gradient) and  $n=10$  (without gradient) experiments. The mean stop zone position lies in the sixth lane ( $56.3 \mu\text{g mL}^{-1}$  ephrinA5) in the steep gradient and in the eighth lane ( $37.5 \mu\text{g mL}^{-1}$  ephrinA5) in the shallow gradient. **b** The stop zone position does not vary between different positions along the naso-temporal axis within the temporal retina. However, at each retinal position, axons stop earlier in steep gradients than in shallow gradients

within 5–20 min [25, 26]. Interestingly, adaptation to ephrinA5 as well as the initial response of growth cones to ephrinA5 seem not to depend on protein synthesis (our own unpublished results). In this respect, ephrinA5 differs from netrin-1 and BDNF [26].

There is no graded responsiveness to in vitro ephrinA5 gradients within the temporal retina

According to general models of retinotectal mapping, temporal axons from the most temporal part of the retina are expected to be more responsive to ephrinA5 than temporal axons from retinal positions close to the optical fissure. To test the responsiveness of temporal axons to ephrinA5 gradients along the temporal-nasal axis, the temporal retina was divided into seven segments ranging from the outer temporal rim of the retina to the optical fissure. Segment t1 corresponds to the nasal-most part of the temporal retina and segment t7 is located at the outer temporal rim of the retina. Axons from all seven segments stop at the same position in the gradient. In the steep gradient, the stop zone positions are t1=117.9±16.4 μm (*n*=4); t2=106.2±15.5 μm (*n*=5); t3=111.9±13.7 μm (*n*=6); t4=105.6±5.4 μm (*n*=7); t5=114.9±7.6 μm (*n*=9); t6=104.5±5.3 μm (*n*=9); and t7=113.6±9.8 μm (*n*=8). Statistical analysis failed to detect any significant difference between the different retinal positions (*P*<0.967 by ANOVA).

The same is true for the shallow gradient, where axons stop at t1=170.2±21.9 μm (*n*=6); t2=149.0±15.8 μm (*n*=7); t3=166.1±13.4 μm (*n*=11); t4=161.4±11.9 μm (*n*=15); t5=151.3±10.1 μm (*n*=16); t6=157.2±12.3 μm (*n*=17); and t7=175.9±15.2 μm (*n*=12) (*P*<0.856 by ANOVA) (Fig. 4b).

Although temporal RGC axons can differentiate between steep and shallow gradients of ephrinA5, they respond to a given gradient as a uniform population independent of their position within the temporal retina and sharply differ from nasal axons, which do not respond to the ephrinA5 gradients. The lack of graded responsiveness of temporal RGC axons has been previously observed in a number of in vitro assays such as the collapse and the stripe assay [24] as well as in discontinuous ephrinA5 gradients produced by μCP [18].

## Conclusions

We used μFNs for the surface design of microscale stepwise graded patterns of the repulsive axon guidance molecule ephrinA5. In contrast to substrate-bound protein gradients produced by μCP, which are built up solely by the geometry of differently sized dots covered with a constant amount of

protein, stepwise gradients fabricated with μFNs consist of lanes covered with increasing ephrinA5 concentrations.

We showed that these substrate-bound repulsive ephrinA5 gradients elicit a stop reaction for temporal RGC axons. In this manner, they clearly differ from diffusible ephrinA5 gradients, which cause growth cone turning or collapse [27]. Moreover, temporal RGC axons can distinguish between stepwise gradients with different slope. In shallow gradients, axons stop after growing further in the gradient, but the ephrinA5 concentration at the stop zone as well as the total amount of ephrinA5 encountered in the gradient are lower than in steep gradients. These findings are consistent with results obtained with discontinuous gradients produced by μCP, which consist of dots or lines covered with a fixed protein concentration but featuring a varying geometry [18]. By contrast, gradients produced by μFN are patterns with a constant geometry but covered with varying protein concentrations. Growth cones can distinguish different slopes in both types of patterns, indicating that they are flexible in “reading” gradients and can detect an increase in protein concentration presented in different ways.

**Acknowledgements** We thank F. Weth for helpful comments on the manuscript. The authors are very grateful for friendly and helpful support from A. Lupas and his department at the Max-Planck-Institute for Developmental Biology in Tuebingen. This work was supported by the DFG (grant 1034/14-1 to M.B. and F.B.) and the DFG Research Center for Functional Nanostructures (CFN, Project E2.3). A.P. receives a stipend from the German National Academic Foundation.

## References

- Dickson BJ (2002) *Science* 298:1959–1964
- Chilton JK (2006) *Dev Biol* 292:13–24
- Sperry RW (1963) *Proc Natl Acad Sci USA* 50:703–710
- Drescher U, Kremoser C, Handwerker C, Lösinger J, Noda M, Bonhoeffer F (1995) *Cell* 82:359–370
- Brown A, Yates PA, Burrola P, Ortuno D, Vaidya A, Jessel TM, O’Leary DDM, Lemke G (2000) *Cell* 102:77–88
- Feldheim DA, Kim YI, Bergemann AD, Frisen J, Barbacid M, Flanagan JG (2000) *Neuron* 25:563–574
- Feldheim DA, Nakamoto M, Osterfield M, Gale NW, DeChiara TM, Rohatgi R, Yancopoulos GD, Flanagan JG (2004) *J Neurosci* 24:2542–2550
- Flanagan JG (2006) *Curr Opin Neurobiol* 16:59–66
- McLaughlin T, O’Leary DDM (2005) *Annu Rev Neurosci* 28:327–355
- Goodhill GJ, Urbach JS (1999) *J Neurobiol* 41:230–241
- Hornberger MR, Duetting D, Ciossek T, Yamada T, Handwerker C, Lang S, Weth F, Huf J, Wessel R, Logan C, Tanaka H, Drescher U (1999) *Neuron* 22:731–742
- Carvalho RF, Beutler M, Marler KJM, Knoell B, Becker-Barroso E, Heintzmann R, Ng T, Drescher U (2006) *Nature Neurosci* 9:322–330
- Lohof AM, Quillan M, Dan Y, Poo M (1992) *J Neurosci* 12:1253–1261

14. Ming GI, Song HJ, Berninger B, Holt CE, Tessier-Lavigne M, Poo MM (1997) *Neuron* 19:1225–1235
15. Davis S, Gale NW, Aldrich TH, Maisonnier PC, Lhotak V, Pawson T, Goldfarb M, Yancopoulos GD (1994) *Science* 266:816–819
16. Egea J, Nissen UV, Dufour A, Sahin M, Greer P, Kullander K, Mrcic-Flogel TD, Greenberg ME, Kiehn O, Vanderhaeghen P, Klein R (2005) *Neuron* 47:515–528
17. Bernard A, Renault JP, Michel B, Bosshard HR, Delamarche E (2000) *Adv Mater* 12:1067–1070
18. von Philipsborn AC, Lang S, Loeschinger J, Bernard A, David C, Lehnert D, Bonhoeffer F, Bastmeyer M (2006) *Development* 133:2487–2495
19. von Philipsborn AC, Lang S, Bernard A, Loeschinger J, David C, Lehnert D, Bonhoeffer F, Bastmeyer M (2006) *Nature Protocols* 1(3)
20. Delamarche E, Bernard A, Schmid H, Michel B, Biebuyck H (1997) *Science* 276:779–781
21. Juncker D, Schmid H, Bernard A, Caelen I, Michel B, Rooij ND, Delamarche E (2001) *J Micromech Microeng* 11:532–541
22. Vielmetter J, Stolze B, Bonhoeffer F, Stuermer CAO (1990) *Exp Brain Res* 8:283–287
23. Walther J, Kern-Veits B, Huf J, Stolze B, Bonhoeffer F (1987) *Development* 101:685–696
24. Monschau B, Kremoser C, Ohta K, Tanaka H, Kaneki T, Yamada T, Handwerker C, Hornberger MR, Lösinger J, Pasquale EB, Siever DA, Verderame MF, Müller BK, Bonhoeffer F, Drescher U (1997) *EMBO J* 16:1258–1267
25. Ming G, Wong ST, Henley J, Yuan X, Song HJ, Spitzer NC, Poo M (2002) *Nature* 417:411–418
26. Piper M, Salih S, Weinl C, Holt CE, Harris WA (2005) *Nature Neurosci* 8:179–186
27. Weinl C, Drescher U, Lang S, Bonhoeffer F, Lösinger J (2003) *Development* 130:1643–1651